Circular output from a high power Nd:YLF slab laser

J. I. Mackenzie[a] and W.A. Clarkson
Optoelectronics Research Centre, University of Southampton, Highfield, Southampton SO17 1BJ, United Kingdom.
[a] jim@orc.soton.ac.uk

ABSTRACT

Neodymium-doped Yttrium Lithium Fluoride (YLF) lasers have traditionally been power-limited by the relatively low tensile strength of the crystal. When power-scaling solid-state lasers, the choice of the gain media geometry, the doping level, and the pumping scheme is dictated by minimizing the impact of thermally induced stress. To date the slab architecture has been the most successful for scaling the average-power of Nd:YLF lasers due to its favorable thermal management. However, for efficient high-radiance laser action it is also necessary to have a good overlap between the cavity mode and the planar gain volume. We present the performance characteristics for an end-pumped slab-laser utilizing a stable low-loss resonator configuration that transforms a circular cavity mode at the output coupler into a very high aspect ratio elliptical beam in the slab gain element to match the pumped volume. The optical arrangement for transforming the beam shape is also suitable for a double-pass slab amplifier configuration.

A polarized CW output power of 50W, on the weaker Nd:YLF 1053nm transition was obtained with a single slab gain element and 110W of incident pump power from three spatially multiplexed diode bars. Laser threshold was around 7W and the slope efficiency, with respect to incident power, 46%.

Keywords: Diode-pumped; End-pumped; Solid-state lasers; Nd:YLF; Resonators

1. INTRODUCTION

New developments in high-average-power lasers are continually emerging, and in recent years, in terms of continuous wave (CW) oscillators and Master Oscillator Power Amplifiers (MOPA's), the merits of high power fiber lasers have outshone other laser architectures [1]. Notwithstanding, the needs of many applications may not always be met by this one architecture alone and new schemes and techniques are often called for that can provide a mode of operation specific to those requirements. For example, in terms of producing high-energy pulses from a solid-state laser system, flash lamp pumping is still the unrivalled champion, despite a relatively low-; repetition rate, lifetime, and wall-plug efficiency, the latter resulting in strong thermo-optical effects associated with the waste excitation energy. The rod geometry well suited to lamp pumping and inherently compatible with symmetric cavity-mode solutions of standard laser resonators, has been the mainstay of the solid-state laser field for several decades. However, steady improvements in the performance of high-power diode lasers, underlies a general shift toward their use in high efficiency, all solid-state lasers, for long-lifetime operation. The rectilinear geometry of the diode laser is inherently compatible with planar active gain media, and therefore simple and efficient coupling schemes are possible. Consequently, the slab geometry is becoming one of the generic power-scaling architectures for bulk gain media [2, 3]. Important for the high-power slab laser architecture is the aspect ratio of the thermal load density within the active material, i.e. quasi-planar, and therefore the pumped volume as this drives the thermal management considerations. Unfortunately though, such a gain distribution is not well suited to the mode solutions of a standard laser resonator, and, for which novel configurations are still of interest. We discuss in this paper one such cavity design, whereby the cavity mode is highly elliptical in one part of the resonator, where the planar gain medium is positioned, and has an aspect ratio of ~1 in another, for example at the output coupling mirror. This novel and stable cavity design can provide an order of magnitude transformation of the cavity-mode aspect ratio; comprising only mirror components for low transmission loss and high laser efficiency, in conjunction with an ability to improve the overlap between pump and signal mode distributions.

As a laser-architecture, the slab geometry is special in that it applicable to a variety of host media, allows the optimization of the active ion concentration and the dimensions of the three independent axes, and therefore, the potential round-trip gain and energy storage capacity. Exploiting these advantages enables efficient high-average-power lasers in either a CW, or pulsed, operational mode. In this theme, we have designed a longitudinally-pumped Neodymium-doped Yttrium Lithium Fluoride (Nd:YLF) slab laser, which has the potential to produce output powers in excess of 100W. Moreover, using the above-mentioned stable cavity to provide an elliptical cavity mode in the planar gain area, we demonstrate efficient extraction of the stored power, simultaneously generating a circular output beam.

2. METHODOLOGY

To explore the capabilities of the beam transformer cavity and performance efficiency of a high-power slab laser, the weaker σ-polarized transition of Nd:YLF was chosen as the test bed. The advantages of this transition and Nd-doped YLF include a weak thermal lens and good spectroscopic properties, well suited to efficient operation in either a CW or pulsed configuration; however, the moderate thermo-mechanical characteristics limit the output powers of typical configurations such as the rod geometry [4].

2.1 Cavity design

The philosophy behind the cavity design is to introduce a high-degree of astigmatism inside the laser resonator such that the aspect ratio of the oscillating mode changes dramatically as a function of position, with low additional loss, and in such a way that the out-coupled radiation is effectively symmetric. In the past, several methods have been reported to achieve a similar outcome, such as intra-cavity anarmorphic prisms or cylindrical optics [5], both refractive components. In its simplest form, the cavity described here requires at least two additional high-reflectivity tilted curved mirrors (A, B in Fig. 1.) in between two end mirrors, and which are aligned in a way that exploits the differential astigmatism arising when *the planes of incidence at each mirror are orthogonal*. That is, for a tilted mirror the effective focal lengths for the orthogonal axes, with respect to the plane of incidence are $f^{\perp}=R\cos(\theta)/2$ and $f^{//}=R/(2\cos(\theta))$, where θ is the incidence angle, and R the mirror radius. Therefore, it is possible to introduce a large change in the aspect ratio of a transmitted beam by rotating the second mirror about the optic axis with respect to the first, such that its plane of incidence is orthogonal, as illustrated in Fig. 1. It is worth noting that in this configuration the beam path does not stay in one plane.

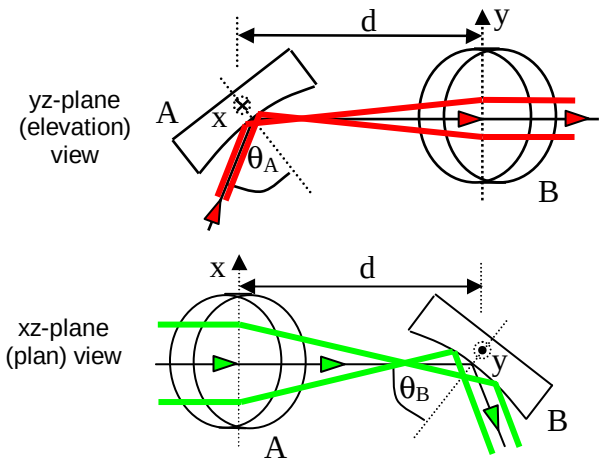

Fig. 1. Two transforming mirrors that introduce a large change in the aspect ratio of a laser beam or cavity mode.

For a paraxial optical system selecting the angles of incidence and mirror radii so that $R_A\sin(\theta_A)\tan(\theta_A)=R_B\sin(\theta_B)\tan(\theta_B)$, implies that the two mirrors (A, B) when separated by, $d=f_A^x+f_B^x=f_A^y+f_B^y$, satisfy the afocal condition for the orthogonal directions simultaneously. The resulting magnification factors in the orthogonal axes are given by; $M^x=f_B^x/f_A^x=(R_A/R_B).(\cos(\theta_A)\cos(\theta_B))$ and $M^y=f_B^y/f_A^y=(R_A/R_B)/(\cos(\theta_A)\cos(\theta_B))$. As such the change in the aspect ratio for the propagating beam is $\cos^2(\theta_A)\cos^2(\theta_B)$. For certain tilt angles therefore, the change in aspect ratio is much larger than can be achieved via techniques employing anamorphic prism pairs or orthogonal cylindrical lens telescopes within the same footprint and with potentially lower losses.

From the above expressions it can be shown that to achieve a reasonable change in aspect ratio, the tilts of the mirrors should be in greater than 50º, at which M_y:M_x = 6:1. At tilt angles of 60º and a paraxial beam, the respective orthogonal beam waists would decrease by a factor of four in the x-axis while increasing by the same factor in the y-axis, as indicated in Fig. 1. A ray-trace model, developed to predict the induced aberrations of the two tilted mirrors, each chosen to have a radius of curvature of 100mm and to be inclined at 60º. The mirrors separated by 125mm and with the beam direction reversed to that shown in Fig. 1, i.e. starting from a circular beam and going to an elliptical one, the induced optical aberrations are less than the diffraction limit for an incident beam radius of up to 1.3mm. Therefore, for a typical cavity mode size of a few hundred microns and longer radii mirrors, aberrations of the tilted mirrors would introduce negligibly small diffraction losses into the cavity. Although this modeling is sufficient for determining the impact of the optical aberrations on a propagating paraxial beam, intra-cavity, the mode is effectively near field and therefore its characteristics should be determined using other methods, such as an ABCD matrix analysis.

Considering one axis at a time, similarities with telescopic resonators, as described by Hanna *et al.* [6], are apparent. Such cavities allow large mode sizes in the gain media by employing an intra-cavity telescope, which can also counter the spherical term of the optical path difference as function of the heat input in the gain element, at least for a certain range of optical powers. However, there are several cavity constraints described in ref [6], which are the same for the beam transforming cavity and essentially has opposing telescopes in the orthogonal axes. Consequently, the cavity solutions must be stable for both axes and the adjustable parameters, mirror curvatures, tilt angles and the spacing of the intra-cavity elements, tailored to provide the desired mode dimensions in the slab and simultaneously a symmetric mode at the output coupler.

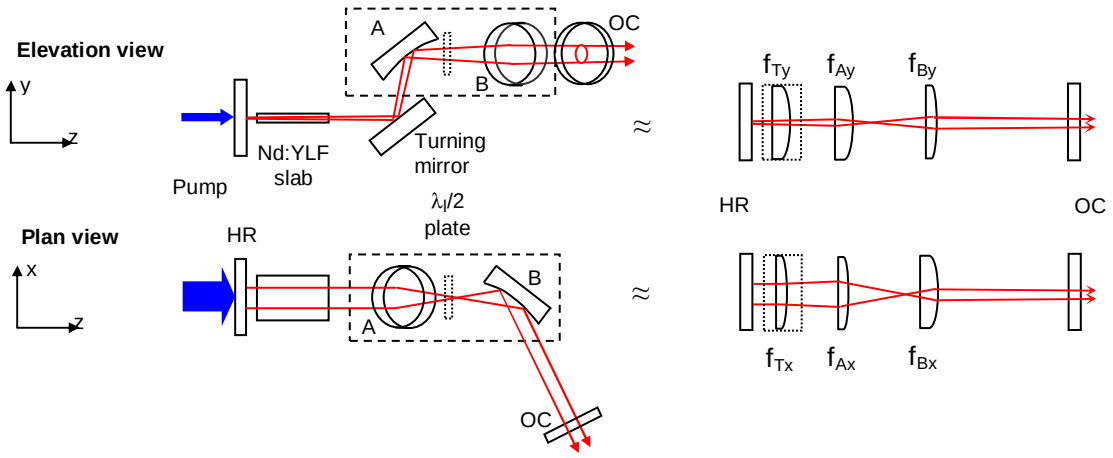

Fig. 2. Schematic of the laser cavity investigated and an equivalent interpretation with thin lenses in place of the intra-cavity mirrors.

2.2 Nd:YLF slab design

As mentioned the chosen gain medium for this demonstration was Nd:YLF, operating on the four-level transition around 1.05µm. To reduce the thermal stress and induced lensing associated with the absorbed pump power, a low doping level was used, i.e. 0.5at.%, for which there is also a small ETU thermal contribution and increased absorption length [4]. In addition, to assist distributing the stress along the length of the active medium in the end-pumped configuration, the Nd:YLF absorption features around 805nm were utilized, as shown in Fig 3. With the additional benefit that high-power laser diodes with a centre wavelength greater than 800nm are readily available. A representation of a typical diode spectrum is shown in Fig. 3, with an arbitrary amplitude to help clarify the graph. A single pass of a 25mm long 0.5at.% Nd:YLF crystal would reduced the pump spectrum to that indicated, corresponding to the respective polarized absorption spectra, that is for the electric field aligned parallel (π-pol) or perpendicular (σ-pol) to the crystal's optic axis (c-axis). As shown, the absorbed power is approximately the same for both polarizations; as such, a polarization coupled pump source may also be employed if desired.

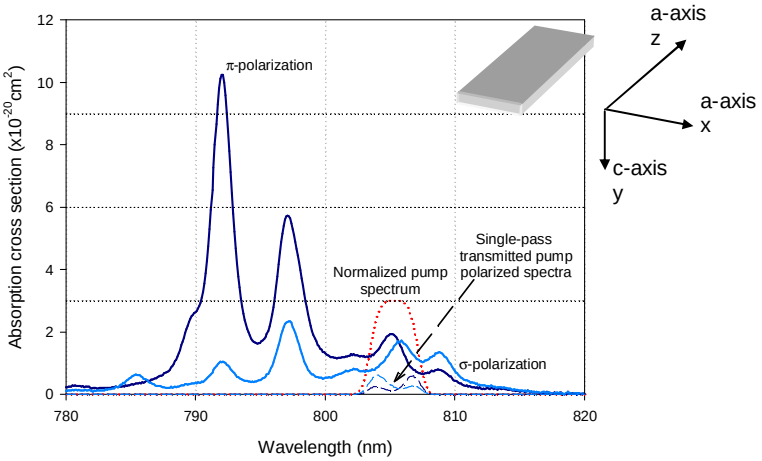

Fig. 3. Nd:YLF polarized absorption spectra, with a normalized example pump spectrum as shown and the calculated single pass power transmission with 86% absorbed by the 25mm crystal length.

A slab with a reasonable aspect ratio that accommodated the beam quality of a three-bar multiplexed diode-laser pump source, which was M^2_y=20 with respect to the fast axis of the diode bars and the thin dimension of the Nd:YLF crystal. Dimensions of the 0.5at.% a-cut Nd:YLF slab were, 1.5mm by 10mm by 25mm with only the end faces of the slab polished to laser quality, the others a fine grind finish to prevent trapped parasitic lasing paths within the gain element. The pump input face was anti-reflection (AR) coated for both the laser and pump wavelengths, while the rear face was AR coated for the laser wavelength and a partial reflector, nominally 65% reflectance, for the pump. Consequently for the diode wavelengths below 808nm, a good proportion of the incident pump, >90%, is absorbed by the crystal.

2.3 Experiment setup

The pump source comprised three 60W (at facet) 30% fill-factor diode bars, collimated in both the fast and slow axes and spatially multiplexed with high reflectance (HR) mirrors. The resulting beam quality was M_x^2 = 370 by M_y^2 = 22 after two orthogonal cylindrical lenses that focused the pump to a beam waist, with radii ω_x = 2.5mm by ω_y = 0.25mm. All three diode bars were mounted on the same water-cooled block and connected in series such that they were driven at the same current level. Each bar had a nominal centre wavelength of 810nm at 25ºC and at high current levels the cooling water temperature had to be <10ºC to obtain the desired pump wavelength of 805nm. The wavelength chirp as a function of the diode current was 0.1nm/A, while the chirp as a function of heat sink temperature was 0.27nm/ºC. Nominally, the Full Width Half Maximum (FWHM) spectral bandwidth at full power was 4.5nm.

Two water-cooled copper heat sinks sandwiched the Nd:YLF slab between them with a thin film Thermal Interface Material (TIM) at each of the largest contact surfaces, providing a low thermal impedance. We positioned the slab with the pump beam central to the aperture of the end faces and the beam waist around the rear end face. It should be noted that the near field image of individual emitters of the diode bars (in the slow axis) occurred approximately 1cm after the beam waist, and therefore well after the crystal had absorbed the majority of the pump-power. Consequently, there was no threat of forming significant “hot spots” within gain medium that could induce localized stress and potential fracture points. Even at the maximum driving current the transmitted pump power through the rear face of the crystal was less than 3W.

In the first experiment we trialed a simple two mirror multi-mode cavity formed with a plano-concave pump in-coupling mirror, radius of curvature (ROC) of 500mm, with >98% transmission at the pump wavelength and >99.5%R for the lasing wavelength. To force the laser to operate on the lower gain, σ-polarized transition at a wavelength of 1053nm, we used an intra-cavity silica Brewster plate 1mm thick and with the plane of incidence aligned to the wider

dimension of the slab, i.e. in the x-z plane of Figures 1-3. A plane-plane output coupler with a reflectance of 77% was used to determine the efficiency of the laser. Changing the output couplers transmission and therefore the total cavity loss, the passive losses in the crystal and mirror coatings were determined to be 0.9%. The cavity length was nominally 80mm.

For the setup of the beam transforming cavity, a plane-plane in-coupling mirror was used, where additional mirrors where introduced as per the schematic in Fig. 3. The plane turning-mirror had a HR coating for 1050nm at an angle of incidence (AOI) between 50º and 65º and light polarized perpendicular to the plane of incidence, the orthogonal polarization was only partially reflected with the reflectance dependent upon the AOI. This mirror coating provided the polarization selectivity within the cavity. A curved mirror with the same coating and ROC = 350mm was mounted "parallel" with the first turning mirror, so that the transmitted beam would lie in the same plane as the incident beam, for the optimum alignment, irrespective of the tilt angle. As illustrated in Fig. 2 another mirror; aligned orthogonal to the first (two), i.e. tilted in the x-z plane, was necessary to complete the beam transformation. Its ROC was 200mm and again coated with the same polarized dielectric mirror as described above. The tilt angles and positions of these mirrors was selected according to a cavity model that used a numerical optimization routine with the beam aspect ratio and dimensions as targeted goals. An additional intra-cavity half-wave plate with the optic axis inclined at 45º to the y-axis, was included between the y-z tilted mirrors and the x-z mirror to ensure that the maximum σ-polarized reflectance for the tilted mirrors and therefore lowest cavity losses.

3. RESULTS

3.1 Laser results

Initial results obtained from the multimode laser cavity are illustrated in Fig. 4. Efficient conversion of the incident diode-pump power was demonstrated for both polarization states, although the intra-cavity Brewster plate introduced significant loss, demonstrated by the lower slope efficiency for the σ-polarized (1053nm) output, with respect to the stronger π-polarized (1047nm) cavity configuration. The maximum power was found for the π-polarized output at 71W with 133W of pump and a 58% slope efficiency, with respect to the incident pump power. The measurement made after a dichroic mirror to separate the residual pump from the laser power. The beam quality was not measured for this cavity configuration, as it was highly multimode, filling out the pumped region to form a highly elliptical profile in the far field. No roll over was observed and the output was limited by the available pump power.

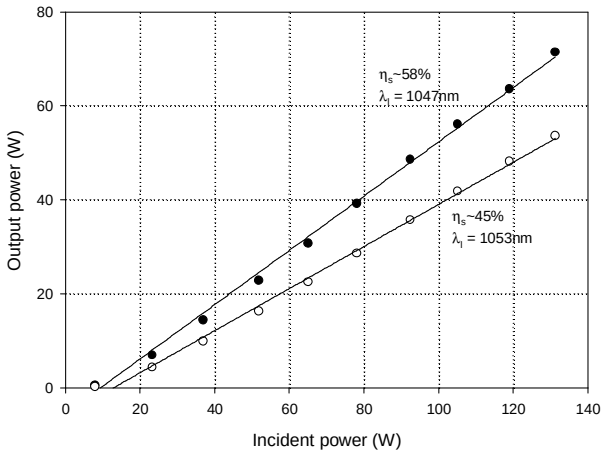

Fig. 4. Multimode Nd:YLF slab laser performance for the two polarization states. σ-polarization (λ_l=1053nm) output selected with a silica Brewster plate with a plane of incidence in the plane of the slab.

For the beam transforming cavity, efficient operation was also observed, as shown in Fig. 5. The spacing of the respective elements were: between in-coupling mirror and slab (d_1), 25mm; the slab to the first curved tilted mirror, A in

Fig. 3, (d_2), 51mm; to the second tilted (orthogonal) mirror, B in Fig. 3, (d_3), 357mm; and finally mirror B to the output coupler mirror (d_4), 285mm. The position of half-wave plate was 60mm from mirror B, and the tilt angles were θ_A=54º and θ_B=57.5º. At a pump power of 111W, which was the maximum available as the wavelength spectrum of the diodes started to change significantly at higher powers, an output power of 50W was measured. The change in the spectral content of the diode pump source was due to feedback from the reflective coating on the back face of the Nd:YLF slab, for which there was sufficient gain at wavelengths outside of the absorption spectrum shown in Fig. 4, i.e. >812nm. Measured with an optical spectrum analyzer, power would shift from the centre of the spectrum around 806nm to satellite peaks at longer wavelengths and the transmitted pump power would increase. We found this problem exacerbated by increased operational hours of the diodes.

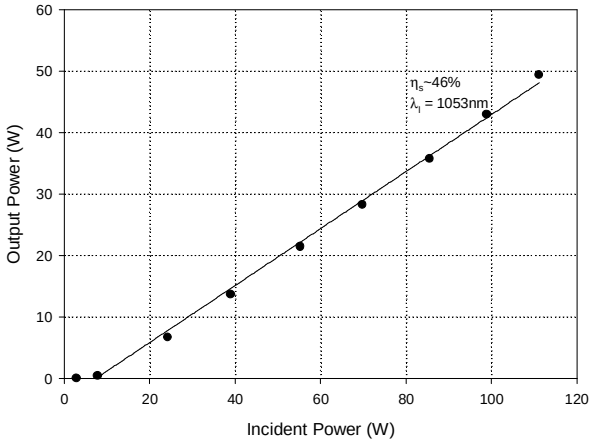

Fig. 5. σ-polarized (λ_l=1053nm) Nd:YLF slab laser performance with beam transformer cavity.

The output beam profile with this cavity configuration was nearly circular, with the beam quality measured at an incident pump power of 55W as M_x^2 = 1.5 by M_y^2 = 1.4 and at the full pump power as M_x^2 = 1.92 by M_y^2 = 1.76. The aspect ratio of the beam on the output coupler was dependent upon the tilted mirror separation but the nominal beam sizes were ω_x=300μm by ω_y=270μm. This configuration was relatively sensitive to the mirror alignment and the thermal load in the gain element was increasing pump power. Other cavity configurations were observed to be less sensitive but the power performance could not be recovered due to further problems with the pump source.

4. DISCUSSION

It is evident that the slab configuration enables high-powers from a single gain element, and that this configuration was well below thermal fracture limits with highly multimode operation approaching the 100W regime. As expected, the π-polarized, 1047nm, output was significantly better than that of the weaker σ-polarized, 1053nm, transition. This is attributed to higher cavity losses for the latter, which would increase for the higher order modes and their greater angular distribution incident upon the Brewster plate for which low loss is only achieved at the Brewster's angle. Threshold values scale well with previously reported values in the literature [4, 7]. Moreover, utilizing a low-doping concentration has meant a distributed heat load and that ETU losses are relatively small and hence do not contribute significantly to the thermal stresses in the laser slab [8]. The strength of the thermal lensing, f_{Tx} and f_{Ty} in Fig. 2, was not investigated but scaling from results published in the literature [4, 9] and calculations of the peak temperature rise in the crystal based on an analytical model for isotropic media described by Hello *et al.*[10]. A peak temperature rise of 25º for 100W of incident pump power is expected, for which the lens in the y-z plane should approach f_{Ty}=1.5m, whereas for the x-z plane, f_{Tx}, should be ~50x weaker.

The beam transformer cavity produced a highly elliptical cavity mode in the slab gain element, providing good extraction efficiency of the absorbed pump power. An optical to optical efficiency of 45% was realized for the weaker Nd:YLF laser transition, which compares extremely well with other reports at this wavelength[4, 11-13]. In fact to the best of our knowledge, this represents the highest average power from a diode-end-pumped near-diffraction-limited Nd:YLF laser. Improvements can be made in terms of the radiance of the output through the beam quality for this particular

cavity configuration. However, there is room for improvement through the mode overlap between the pump and laser fields, as well as engineering the thermal and gain distribution in the x-axis.

An ABCD matrix model developed to determine the cavity mode dimensions throughout the resonator, in the orthogonal axes as defined by the slab in Fig. 3, predicted beam dimensions, in the case of the cavity configurations described in section 3.1, as displayed in Fig. 6. It is evident that there is a good overlap of the pumped region and the laser mode, as highlighted by the shaded boxes, although the pump widths indicated are only the beam waists and not the average beam size over the full length of the slab. Notwithstanding, the mode size in the slab has an aspect ratio of 1:15, where as at the output coupler it is nearly 1:1. Note in the model, the beam quality for each axis is assumed to be diffraction-limited. Allowing for contributions from higher order modes would provide larger mode sizes that fill out the gain distribution available.

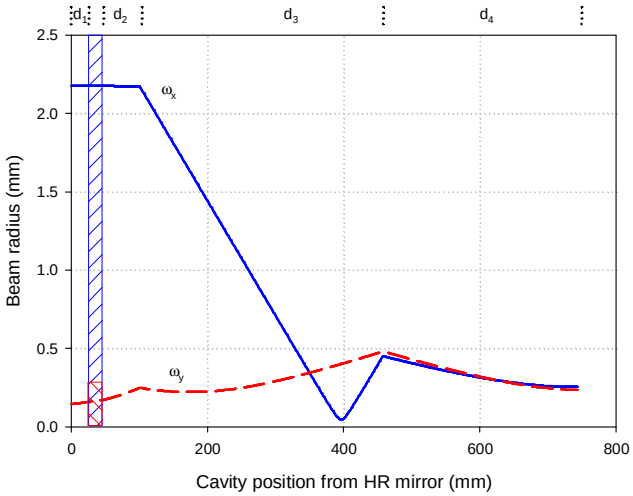

Fig. 6. Theoretical mode size as a function of the cavity position for the configuration discussed in section 3.1. Shaded regions indicate pump beam size in the slab, /// in the x-z plane and \\\ in the y-z plane.

Comparing the slope efficiency between the multi-mode and nearly single mode 1053nm lasers, we see a slightly improved performance for the latter. The additional round trip cavity loss 1.5% associated with the tilted mirrors and half-wave plate is considerably lower than the output coupling transmission and should have a relatively small effect on the slope efficiency. Whereas for the multi-mode cavities, the drop in slope efficiency associated with the Brewster plate, indicates additional losses of 4% per round trip. Instead the mode-matching efficiency, or the dS/dF factor [14, 15], for a top-hat pump distribution, which is similar to the case here, starts low, near threshold, and increases until it saturates when the laser is operating at several times threshold, even for four-level transitions with no reabsorption losses. Hence the similar performance of the multi-mode laser and that with the beam transformer cavity can be attributed to the difference in mode-matching efficiency, despite the lower round trip cavity losses.

5. CONCLUSIONS

In this paper we have presented a high power end-pumped Nd:YLF slab laser, which in a multi-mode configuration generated >70W in CW output power polarized output at a wavelength of 1047nm and 55W at a wavelength of 1053nm. Utilizing a novel laser resonator that provides an order of magnitude change in the aspect ratio of the intracavity mode, we obtained 50W of laser output on the σ-polarized transition with good beam quality. Excellent conversion efficiency and the high average-power demonstrate that this concept is ideally suited to planar gain media with highly elliptical gain distributions, fully exploiting the thermal advantages of this geometry. This approach opens the way for power-scalable solutions, which are applicable to lasers with diverse modes of operations, from the CW to pulsed regime.

REFERENCES

1. A. Tunnermann, T. Schreiber, F. Roser, A. Liem, S. Hofer, H. Zellmer, S. Nolte, and J. Limpert, "The renaissance and bright future of fibre lasers," *Journal Of Physics B-Atomic Molecular And Optical Physics* **38**(9), S681-S693 (2005).
2. T. S. Rutherford, W. M. Tulloch, E. K. Gustafson, and R. L. Byer, "Edge-pumped quasi-three-level slab lasers: Design and power scaling," *IEEE Journal Of Quantum Electronics* **36**(2), 205-219 (2000).
3. G. D. Goodno, C. P. Asman, J. Anderegg, S. Brosnan, E. C. Cheung, D. Hammons, H. Injeyan, H. Komine, W. H. Long, M. McClellan, S. J. McNaught, S. Redmond, R. Simpson, J. Sollee, M. Weber, S. B. Weiss, and M. Wickham, "Brightness-scaling potential of actively phase-locked solid-state laser arrays," *IEEE Journal of Selected Topics in Quantum Electronics* **13**(3), 460-472 (2007).
4. X. Y. Peng, L. Xu, and A. Asundi, "High-power efficient continuous-wave TEM_{00} intracavity frequency-doubled diode-pumped Nd:YLF laser," *Applied Optics* **44**(5), 800-807 (2005).
5. W. Koechner, *Solid State Laser Engineering - Chapter 5*, 4th ed., Springer Series in Optical Sciences (Springer Verlag, Berlin Heidelberg, 1999), Vol. 1, p. 740.
6. D. C. Hanna, C. G. Sawyers, and M. A. Yuratich, "Telescopic Resonators for Large-Volume Tem_{00}-Mode Operation," *Optical and Quantum Electronics* **13**(6), 493-507 (1981).
7. P. J. Hardman, W. A. Clarkson, G. J. Friel, M. Pollnau, and D. C. Hanna, "Energy-transfer upconversion and thermal lensing in high-power end-pumped Nd:YLF laser crystals," *IEEE Journal of Quantum Electronics* **35**(4), 647-655 (1999).
8. W. A. Clarkson, "Thermal effects and their mitigation in end-pumped solid-state lasers," *Journal of Physics D-Applied Physics* **34**(16), 2381-2395 (2001).
9. C. Pfistner, R. Weber, H. P. Weber, S. Merazzi, and R. Gruber, "Thermal beam distortions in end-pumped Nd:YAG, Nd:GSGG, and Nd:YLF rods," *IEEE Journal of Quantum Electronics* **30**(7), 1605 (1994).
10. P. Hello, E. Durand, P. K. Fritschel, and C. N. Man, "Thermal Effects in Nd:YAG Slabs 3D Modeling and Comparison with Experiments," *Journal of Modern Optics* **41**(7), 1371-1390 (1994).
11. W. A. Clarkson, P. J. Hardman, and D. C. Hanna, "High-power diode-bar end-pumped Nd:YLF laser at 1.053μm," *Optics Letters* **23**(17), 1363-1365 (1998).
12. Y. Hirano, T. Yanagisawa, S. Ueno, T. Tajime, O. Uchino, T. Nagai, and C. Nagasawa, "All-solid-state high-power conduction-cooled Nd:YLF rod laser," *Optics Letters* **25**(16), 1168-1170 (2000).
13. A. Dergachev, J. H. Flint, Y. Isyanova, B. Pati, E. V. Slobodtchikov, K. F. Wall, and P. F. Moulton, "Review of multipass slab laser systems," *IEEE Journal of Selected Topics in Quantum Electronics* **13**(3), 647-660 (2007).
14. W. P. Risk, "Modeling of Longitudinally Pumped Solid-State Lasers Exhibiting Reabsorption Losses," *Journal of the Optical Society of America B-Optical Physics* **5**(7), 1412-1423 (1988).
15. T. Taira, W. M. Tulloch, and R. L. Byer, "Modeling of quasi-three-level lasers and operation of cw Yb:YAG lasers," *Applied Optics* **36**(9), 1867-1874 (1997).